HHS Public Access

Author manuscript

J Am Chem Soc. Author manuscript; available in PMC 2022 January 13.

Published in final edited form as:

J Am Chem Soc. 2021 January 13; 143(1): 137–141. doi:10.1021/jacs.0c12414.

Origin of Free Energy Barriers of Decarboxylation and the Reverse Process of CO_2 Capture in Dimethylformamide and in Water

Shaoyuan Zhou[1,2], **Bach T. Nguyen**[3], **John P. Richard**[4], **Ronald Kluger**[5], **Jiali Gao**[1,3]

[1]Institute of Systems and Physical Biology, Shenzhen Bay Laboratory, Shenzhen 581055, China;

[2]Institute of Theoretical Chemistry, Jilin University, Changchun 100231, China;

[3]Department of Chemistry and Supercomputing Institute, University of Minnesota, Minneapolis, MN 55455, USA;

[4]Department of Chemistry, State University of New York at Buffalo, Buffalo, NY 47907, USA;

[5]Department of Chemistry, University of Toronto, Toronto, Ontario M5S 3H6, Canada

Abstract

In aqueous solution, biological decarboxylation reactions proceed irreversibly to completion, whereas the reverse carboxylation processes are typically powered by the hydrolysis of ATP. The exchange of the carboxylate of ring-substituted arylacetates with isotope-labeled CO_2 in polar aprotic solvents reported recently suggests a dramatic change in the partition of reaction pathways. Yet, there is little experimental data pertinent to the kinetic barriers for protonation, and thermodynamic data on CO_2 capture by the carbanions of decarboxylation reactions. Employing a combined quantum mechanical and molecular mechanical simulation approach, we investigated the decarboxylation reactions of a series of organic carboxylate compounds in aqueous and in dimethylformamide solutions, revealing that the reverse carboxylation barriers in solution are fully induced by solvent effects. A linear Bell-Evans-Polanyi relationship was found between the rates of decarboxylation and the Gibbs energies of reaction, indicating diminishing recombination barriers in DMF. In contrast, protonation of the carbanions by the DMF solvent has large free-energy barriers, rendering the competing exchange of isotope-labeled CO_2 reversible in DMF. The

Corresponding Authors: **Jiali Gao** – Institute of Systems and Physical Biology, Shenzhen Bay Laboratory, Shenzhen 581055, China; Beijing University Shenzhen Graduate School, Shenzhen 581055, China; Department of Chemistry and Supercomputing Institute, University of Minnesota, Minneapolis, MN 55455, USA; gao@jialigao.org, **John P. Richard** – Department of Chemistry, State University of New York at Buffalo, Buffalo, NY 47907, USA; jrichard@buffalo.edu, **Ronald Kluger** – Department of Chemistry, University of Toronto, Toronto, Ontario M5S 3H6, Canada; r.kluger@utoronto.ca.
Shaoyuan Zhou – Institute of Theoretical Chemistry, Jilin University, Changchun 100231, China; Institute of Systems and Physical Biology, Shenzhen Bay Laboratory, Shenzhen 581055, China;
Bach T. Nguyen – Department of Chemistry and Supercomputing Institute, University of Minnesota, Minneapolis, MN 55455, USA;
Author Contributions
JG, JPR and RK designed the research, SZ, BTN, and JG performed the calculations and analyses. The manuscript was written through contributions of all authors. All authors have given approval to the final version of the manuscript.

Supporting Information
A summary of computational methods, reaction schemes, computed potentials of mean force and solvation free energies for all reactions and optimized stationary and transition state structures (24 pages, PDF). This material is available free of charge via the Internet at http://pubs.acs.org.

The authors declare no competing financial interest.

finding of an intricate interplay of carbanion stability and solute-solvent interaction in decarboxylation and carboxylation could be useful to designing novel materials for CO_2 capture.

Graphical Abstract

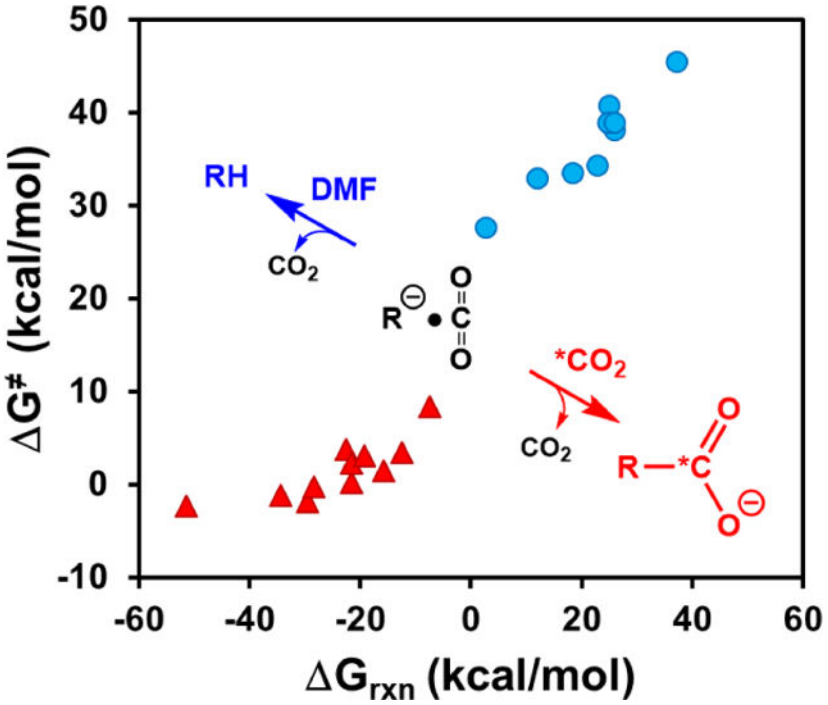

In aqueous solution, enzymatic decarboxylations, such as that of orotidine monophosphate (OMP) catalyzed by OMP decarboxylase, proceed effectively irreversibly to 100% completion,[1, 2] while biosynthetic carboxylation reactions are coupled to thermodynamically favorable processes, particularly the hydrolysis of ATP. In Nature, the equilibrium of decarboxylation and carboxylation is established through CO_2 release by respiring organisms and CO_2 fixation in photosynthesis on a mammoth scale of billions of tons per year.[3] Although the change from water to aprotic solvents can accelerate decarboxylation reactions,[4] we were intrigued by reports[5, 6] that exchange between the carboxylate of ring-substituted arylacetates (R-CO_2^-, Scheme 1) and labeled $^{13}CO_2$ or $^{14}CO_2$ in polar aprotic solvents dimethylformamide (DMF) or dimethylsulfoxide (DMSO) is substantially faster than their decarboxylation to form substituted toluenes (RH).[5–11] These reaction conditions dramatically change the course of decarboxylation. Scheme 1 shows partitioning of the carbanion intermediate $R^-\ldots CO_2$ of decarboxylation of $R^-\ldots CO_2$ among recombination to form the reactant (k_{-1}), protonation to form a ring-substituted toluene (k'_p), and diffusional separation (k_{-d}) to form a free carbanion, which then partitions between protonation (k_p) and addition of isotope-labelled *CO_2. Other competing patyways include a nucleophilic addition to the solvent DMF and a disproportionation process of arylacetates;[5, 6] they have high reaction barriers (SI) and are not further discussed in this study. The observation of exchange of *CO_2 requires a large kinetic barrier to protonation of ring substituted benzyl carbanions, compared to the barrier for addition of CO_2: k_d[*CO_2]>> k'_p, k_p. However,

there is little experimental data pertinent to the kinetic barriers for protonation of ring-substituted benzyl carbanions by DMF or DMSO,[12–14] and no data for addition of these carbanions to CO_2. We report here the results of a combined quantum mechanical and molecular mechanical (QM/MM) simulation study to determine the relative barriers to partitioning a series of carbanions between addition to CO_2 and protonation by DMF.

We carried out molecular dynamics simulations to determine the potentials of mean force (PMF) along the CO_2 dissociation coordinate for a set of 11 organic acids in water and in DMF, employing a dual-level QM/MM potential[15, 16] to yield results at a quality of density functional theory with the M06-2X/aug-cc-pVTZ functional.[17] The PMF for six decarboxylation reactions in DMF and in aqueous solution are depicted in Figure 1, along with the free energy profiles in the gas phase for comparison. The remaining data and details are given in the SI. The experimental free-energy barriers are obtained from rate constants mostly extrapolated to ambient temperature,[18] whereas free energies of reaction are taken from the analysis by Guthrie.[18,19] For the nine reactions where experimental data are available, the root-mean-square-errors (RMSE) between experiment and computation are 4.4 and 6.1 kcal/mol, respectively, for the barrier height and reaction free energy (Table S1), and the mean-signed-errors (MSE) are smaller (0.3 and 1.2 kcal/mol) than unsigned errors and RMSE. The agreement is good in view of the large span of rates and free energies. Quantitative rate constants for decarboxylation reactions in DMF are scarce,[20] but in view of the good accord for the aqueous data and linear free energy relationships discussed below, the results demonstrate that the present simulations are adequate to provide insights on the origin of solvent effects on these decarboxylation reactions.

First, decarboxylation reactions in water typically have high free energy barriers accompanied by strong solvation effects,[4, 20–23] occurring at elevated temperatures. This is due to greater reactant stabilization by aqueous solvation relative to that at the decarboxylation transition state.[22, 23] This effect is especially dramatic in the reverse, carboxylation process, and clearly depicted in Figures 1 and S2. In the gas phase, there is no or little recombination barrier for CO_2 capture, but in contrast, aqueous solvation induces substantial free-energy barriers to CO_2 recombination in all decarboxylation reactions. For nitroacetate ion, the recombination barrier is as large as 17 kcal/mol in water, reflecting an unusual Brønsted relationship between the rate and equilibrium constants for deprotonation, called nitroalkane anomaly.[24, 25] Both deprotonation and decarboxylation reactions yield the same carbanion intermediate, with slow re-hybridization of the charge localized carbanion.[26] It is remarkable that this phenomenon is carried over to the decarboxylation reaction. In protic solvents, protonation of the transient carbanion intermediate $R^-\ldots CO_2$ to form RH (Scheme 1) renders decarboxylation reactions effectively irreversible. Consequently, in aqueous solution, the partition of $R^-\ldots CO_2$ in Scheme 1 favors formation of RH because of the weak carbon acidity of the decarboxylation product. In DMF, the free energy barriers to CO_2 recombination are much smaller than those in water (Figure 1). For several reactions, the overall free energy barriers of the recombination process are below the product state of decarboxylation or without a barrier at all. Overall, Figure 1 reveals that solvent reorganization, created by desolvation as the reacting species approach each other to form a chemical bond, induces CO_2 recombination barriers, and the solvation-induced barriers are substantially smaller in DMF than in aqueous solution.

Secondly, we have examined the partition between CO_2 recombination and protonation of the carbanions of decarboxylation by proton abstraction from DMF. For the latter calculations, we employed M06-2X/aug-cc-pVTZ along with the Minnesota solvation model.[27] The method was validated by comparison between the computed gas-phase basicities and the experimental data,[28] with an RMSE of 2.0 kcal/mol. The thermodynamic driving forces and free energy barriers for the proton transfer and CO_2 recombination reactions are listed in Table 1. Except phenyl anion, all carbanions have smaller gas-phase basicity than DMF (385.9 kcal/mol) and exhibit positive free energies of reaction. On the other hand, the carboxylation reactions are substantially favorable both in the gas phase and in solution. Furthermore, proton abstraction from DMF by the carbanions of decarboxylation have large free-energy barriers, typically greater than 30 kcal/mol, in sharp contrast to the small barriers for CO_2 recapture in DMF (Table 1). Therefore, the partition (Scheme 1) is strongly favored to the carboxylation process over protonation to form toluene derivatives in DMF.

The rate of decarboxylation reactions in water are known to correlate with the pKa values of the conjugate acids of the anions of decarboxylation through Brønsted plots at 25 °C.[29] Interestingly, Shock and coworkers showed that a Brønsted plot of decarboxylation at 300 °C is also correlated with the pKa at 25 °C,[30] suggesting that the use of rate extrapolation to ambient temperature is reasonable.[29] Here, we found that the decarboxylation rates both in water and in DMF fall in a linear Bell-Evans-Polanyi plot. Figure 2 shows that the agreement between experiments and computation for the decarboxylation reactions in water is excellent, yielding a slope of 0.71 and 0.76, respectively. The intercept in the experimental correlation (16.7 kcal/mol) is 1.6 kcal/mol greater than that of computational data (15.0 kcal/mol). The Bell-Evans-Polanyi relationship for the decarboxylation reactions in DMF solution gives a slightly increased slope (0.79) and markedly reduced intercept (6.6 kcal/mol). In physical organic chemistry, the slope of a Bell-Evans-Polanyi plot correlates with the transition state along the reaction pathway.[31] As there is no free energy barrier for the carboxylation process in the gas phase, this limiting case implies a slope of unity and zero intercept. The small increase in slope in DMF relative to that in water is significant, indicating further advancement of the transition state in an aprotic solvent. The smaller intercept value in DMF solution than aqueous solution corresponds to weak solvent reorganization and, thus, smaller solvation-induced free-energy barrier. Indeed, the average solvent-induced recombination barrier height is only 1.5 kcal/mol above the decomposition products, whereas it is 8.8 (9.6) kcal/mol in water from computation (experiments).

Finally, the average recombination barriers in aqueous and DMF solutions are not without trends. Figure 3 depicts the computed barriers for CO_2 capture by the anionic nucleophiles of decarboxylation against the free energies of reaction. Interestingly, greater barriers are found to accompany smaller overall endergonicity in both solvents with similar slopes (−0.21 and −0.24 in DMF and in water). In dry DMF, a solvent favoring CO_2 capture, recombination barriers are absent when decarboxylation reactions become highly endergonic (Figure 3). In other words, the free energy cost for a spontaneous decarboxylation reaction is largely dictated by the intrinsic, i.e., gas-phase, free energy of decarboxylation. Nevertheless, the Bell-Evans-Polanyi plot does not show direct correlation of the rates of decarboxylation or CO_2 recombination with the Gibbs energy of reaction in the gas phase. It

is the combined effects of the intrinsic stability of the carbanions and intermolecular interactions that lead to a highly correlated linear regression ($R_2 \geq 0.95$).

The reversibility of decarboxylation and carboxylation was reported in the synthesis of α-nitro acids in methanol under basic and saturating CO_2 conditions.[32] Falvey and coworkers,[8, 9] and others,[33, 34] showed that decarboxylation of zwitterionic imidazolium-2-carboxylate is reversible by $^{13}CO_2$ exchange in aprotic solvents, but protonation of the decarboxylation product in solvent mixtures containing a proton source inhibits the recovery of the carboxylate starting material. These N-heterocyclic carbene materials have been used for a variety of applications, including organic synthesis and CO_2-transfer agents.[35] Wolfenden and coworkers found a modest rate enhancement by transferring N-methyl orotate from water to DMF,[20] in accord with the present results. Mayr and coworkers investigated a range of nucleophilic addition of carbanions to heteroallenes.[36] Recently, a number of groups reported reversible exchange reactions of spontaneous decarboxylation and carboxylation of organic acids.[5–11] Decarboxylation reactions are inherently slow, typically carried out at high temperatures.[30] The Bell-Evans-Polanyi relationship in Figure 2 reveals that a balanced act of both carbanion stabilization to increase the overall decarboxylation rate and solvation effects to facilitate deprotonation of the conjugate acid of the decarboxylation anion may be considered in designing materials for CO_2 capture, storage and release.[34, 37] An organic solvent favors CO_2 capture, but it would be of interest to balance carbanion stability and solvation effects to carry out reversible decarboxylation and CO_2 capture in the presence of water.

In summary, the present study reveals that the barrier for CO_2 capture corresponding to the reverse decarboxylation reaction is fully induced by solvent effects, especially in aqueous solution. The rates of decarboxylation in water and in DMF fall linearly to the Bell-Evans-Polanyi relationship, revealing diminishing recombination free-energy barriers in DMF relative to aqueous solution. For CO_2 capture, the recombination reaction has an average solvent-induced free energy barrier of nearly 10 kcal/mol in water, and less than 2 kcal/mol in DMF. In contrast, protonation of the carbanions by the DMF solvent has large free-energy barriers, typically greater than 30 kcal/mol, rendering the competing diffusion and exchange of isotope-labeled CO_2 reversible in DMF. Therefore, in DMF, the partition of the carbanions in Scheme 1 favors recombination with a CO_2 molecule.

Supplementary Material

Refer to Web version on PubMed Central for supplementary material.

ACKNOWLEDGMENT

The computations were performed at the Supercomputing Center of Shenzhen Bay Laboratory, and completed at the Minnesota Supercomputing Institute.

Funding Sources

This work was partially supported by Shenzhen Municipal Science and Technology Innovation Commission (KQTD2017-0330155106581) and part of the study was completed at Minnesota, which is supported by the National Institutes of Health (GM046736). The work at Buffalo has been supported by the NIH (GM134881).

ABBREVIATIONS

DL	dual level
DMF	dimethylformamide
DMSO	dimethyl sulfoxide
MSE	mean signed errors
OMP	orotidine monophosphate
PMF	potential of mean force
QM/MM	quantum mechanical and molecular mechanical
RMSE	root-mean-square errors
SI	supporting information

REFERENCES

1. Richard JP; Amyes TL; Reyes AC, Orotidine 5 ’-Monophosphate Decarboxylase: Probing the Limits of the & IT; Possible & IT; for Enzyme Catalysis. Acc. Chem. Res 2018, 51, 960–969. [PubMed: 29595949]
2. Radzicka A; Wolfenden R, A proficient enzyme. Science 1995, 267, 90–3. [PubMed: 7809611]
3. Walsh CT, Biologically generated carbon dioxide: nature’s versatile chemical strategies for carboxy lyases. Nat. Prod. Rep 2020, 37, 100–135. [PubMed: 31074473]
4. Kemp DS; Paul K, Decarboxylation of Benzisoxazole-3-Carboxylic Acids - Catalysis by Extraction of Possible Relevance to Problem of Enzymatic Mechanism. J. Am. Chem. Soc 1970, 92, 2553–4.
5. Kong DY; Moon PJ; Lui EKJ; Bsharat O; Lundgren RJ, Direct reversible decarboxylation from stable organic acids in dimethylformamide solution. Science 2020, 369, 557. [PubMed: 32554626]
6. Destro G; Horkka K; Loreau O; Buisson DA; Kingston L; Del Vecchio A; Schou M; Elmore CS; Taran F; Cantat T; Audisio D, Transition-Metal-Free Carbon Isotope Exchange of Phenyl Acetic Acids. Angew. Chem. Int. Ed 2020, 59, 13490–13495.
7. Kluger R, Decarboxylation, CO_2 and the Reversion Problem. Acc. Chem. Res 2015, 48, 2843–2849. [PubMed: 26528892]
8. Denning DM; Falvey DE, Solvent-Dependent Decarboxylation of 1,3-Dimethylimdazolium-2-Carboxylate. J. Org. Chem 2014, 79, 4293–4299. [PubMed: 24762208]
9. Denning DM; Falvey DE, Substituent and Solvent Effects on the Stability of N-Heterocyclic Carbene Complexes with CO_2. J. Org. Chem 2017, 82, 1552–1557. [PubMed: 28067512]
10. Hinsinger K; Pieters G, The Emergence of Carbon Isotope Exchange. Angew Chem Int Edit 2019, 58, 9678–9680.
11. Destro G; Loreau O; Marcon E; Taran F; Cantat T; Audisio D, Dynamic Carbon Isotope Exchange of Pharmaceuticals with Labeled CO_2. J. Am. Chem. Soc 2019, 141, 780–784. [PubMed: 30586301]
12. Llauger L; Cosa G; Scaiano JC, First determination of absolute rate constants for the reaction of aroyl-substituted benzyl carbanions in water and DMSO. J. Am. Chem. Soc 2002, 124, 15308–15312. [PubMed: 12487606]
13. Llauger L; Miranda MA; Cosa G; Scaiano JC, Comparative study of the reactivities of substituted 3-(benzoyl)benzyl carbanions in water and in DMSO. J. Org. Chem 2004, 69, 7066–7071. [PubMed: 15471454]

14. Haussermann A; Rominger F; Straub BF, CO_2 on a Tightrope: Stabilization, Room-Temperature Decarboxylation, and Sodium-Induced Carboxylate Migration. Chem-Eur J 2012, 18, 14174–14185. [PubMed: 22997025]
15. Gao J, Hybrid Quantum Mechanical/Molecular Mechanical Simulations: An Alternative Avenue to Solvent Effects in Organic Chemistry. Acc. Chem. Res 1996, 29, 298–305.
16. Gao J, Enzymatic Kinetic Isotope Effects from Path-Integral Free Energy Perturbation Theory. Methods Enzymol 2016, 577, 359–388. [PubMed: 27498645]
17. Zhao Y; Truhlar DG, M06 DFT functionals. Theor. Chem. Acc 2008, 120, 215.
18. Guthrie JP; Peiris S; Simkin M; Wang Y, Rate constants for decarboxylation reactions calculated using no barrier theory. Can. J. Chem 2010, 88, 79–98.
19. Gao D; Pan Y-K, A QM/MM Monte Carlo Simulation Study of Solvent Effects on the Decarboxylation Reaction of N-Carboxy-2-imidazolidinone Anion in Aqueous Solution. J. Org. Chem 1999, 64, 1151–1159.
20. Lewis CA; Wolfenden R, Orotic Acid Decarboxylation in Water and Nonpolar Solvents: A Potential Role for Desolvation in the Action of OMP Decarboxylase. Biochemistry 2009, 48, 8738–8745. [PubMed: 19678695]
21. Crosby J; Stone R; Lienhard GE, Mechanisms of Thiamine-Catalyzed Reactions - Decarboxylation of 2-(1-Carboxy-1-Hydroxyethyl)-3,4-Dimethylthiazolium Chloride. J. Am. Chem. Soc 1970, 92, 2891–2900. [PubMed: 5439974]
22. Gao J, An Automated Procedure for Simulating Chemical Reactions in Solution. Application to the Decarboxylation of 3-Carboxybenzisoxazole in Water. J. Am. Chem. Soc 1995, 117, 8600–7.
23. Lin Y.-l.; Gao J, Kinetic Isotope Effects of L-Dopa Decarboxylase. J. Am. Chem. Soc 2011, 133, 4398–4403. [PubMed: 21366322]
24. Kresge AJ, Nitroalkane anomaly. Can. J. Chem 1974, 52, 1897–903.
25. Bernasconi CF, The principle of nonperfect synchronization: more than a qualitative concept? Acc. Chem. Res 1992, 25, 9–16.
26. Major DT; York DM; Gao J, Solvent Polarization and Kinetic Isotope Effects in Nitroethane Deprotonation and Implications to the Nitroalkane Oxidase Reaction. J. Am. Chem. Soc 2005, 127, 16374–16375. [PubMed: 16305206]
27. Frisch MJ; Trucks GW; Schlegel HB; Scuseria GE; Robb MA; Cheeseman JR; Scalmani G; Barone V; Petersson GA; Nakatsuji H; Li X; Caricato M; Marenich AV; Bloino J; Janesko BG; Gomperts R; Mennucci B; Hratchian HP; Ortiz JV; Izmaylov AF; Sonnenberg JL; Williams; Ding F; Lipparini F; Egidi F; Goings J; Peng B; Petrone A; Henderson T; Ranasinghe D; Zakrzewski VG; Gao J; Rega N; Zheng G; Liang W; Hada M; Ehara M; Toyota K; Fukuda R; Hasegawa J; Ishida M; Nakajima T; Honda Y; Kitao O; Nakai H; Vreven T; Throssell K; Montgomery JA Jr.; Peralta JE; Ogliaro F; Bearpark MJ; Heyd JJ; Brothers EN; Kudin KN; Staroverov VN; Keith TA; Kobayashi R; Normand J; Raghavachari K; Rendell AP; Burant JC; Iyengar SS; Tomasi J; Cossi M; Millam JM; Klene M; Adamo C; Cammi R; Ochterski JW; Martin RL; Morokuma K; Farkas O; Foresman JB; Fox DJ Gaussian 16, A.03; Wallingford, CT, 2016.
28. NIST NIST Chemistry WebBook. (accessed October 7).
29. Wolfenden R; Lewis CA; Yuan Y, Kinetic Challenges Facing Oxalate, Malonate, Acetoacetate, and Oxaloacetate Decarboxylases. J. Am. Chem. Soc 2011, 133, 5683–5685. [PubMed: 21434608]
30. Glein CR; Gould IR; Lorance ED; Hartnett HE; Shock EL, Mechanisms of decarboxylation of phenylacetic acids and their sodium salts in water at high temperature and pressure. Geochim. Cosmochim. Acta 2020, 269, 597–621.
31. Ritchie CD, Physical Organic Chemistry: The Fundmental Concepts. 2nd. ed.; CRC Press.: New York, 1989; p 376.
32. Finkbeiner HL; Stiles M, Chelation as a Driving Force in Organic Reactions .4 Synthesis of Alpha-Nitro Acids by Control of Carboxylation-Decarboxylation Equilibrium. J. Am. Chem. Soc 1963, 85, 616–22.
33. Voutchkova AM; Feliz M; Clot E; Eisenstein O; Crabtree RH, Imidazolium carboxylates as versatile and selective N-heterocyclic carbene transfer agents: Synthesis, mechanism, and applications. J. Am. Chem. Soc 2007, 129, 12834–12846. [PubMed: 17900114]

34. Fevre M; Pinaud J; Leteneur A; Gnanou Y; Vignolle J; Taton D; Miqueu K; Sotiropoulos JM, Imidazol(in)ium Hydrogen Carbonates as a Genuine Source of N-Heterocyclic Carbenes (NHCs): Applications to the Facile Preparation of NHC Metal Complexes and to NHC-Organocatalyzed Molecular and Macromolecular Syntheses. J. Am. Chem. Soc 2012, 134, 6776–6784. [PubMed: 22455795]

35. Kayaki Y; Yamamoto M; Ikariya T, N-Heterocyclic Carbenes as Efficient Organocatalysts for CO_2 Fixation Reactions. Angew. Chem. Int. Edit 2009, 48, 4194–4197.

36. Li Z; Mayer RJ; Ofial AR; Mayr H, From Carbodiimides to Carbon Dioxide: Quantification of the Electrophilic Reactivities of Heteroallenes. J. Am. Chem. Soc 2020, 142, 8383–8402.

37. Long YD; Fang Z, Hydrothermal conversion of glycerol to chemicals and hydrogen: review and perspective. Biofuel Bioprod Bior 2012, 6, 686–702.

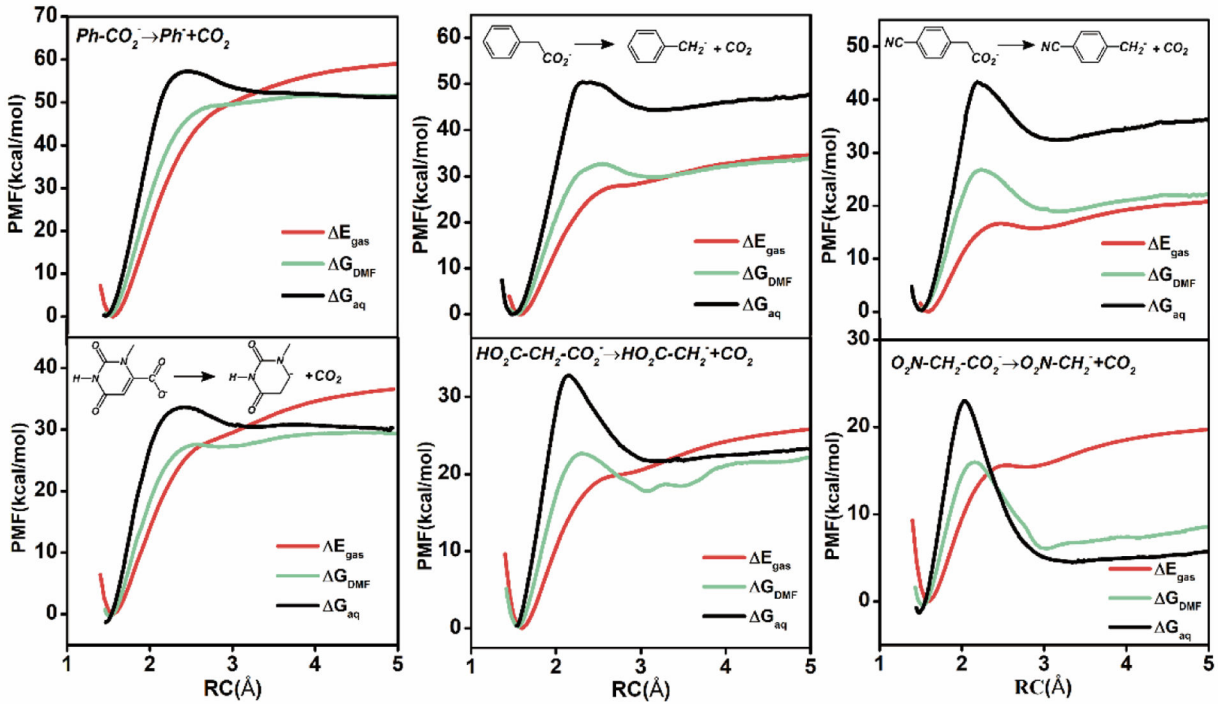

Figure 1.

Computed potential of mean force for decarboxylation reactions in the gas phase (red), aqueous solution (black), and dimethylformamide (green) along the distance coordinate between the carbon atom of the carboxylate and the carbanion site.

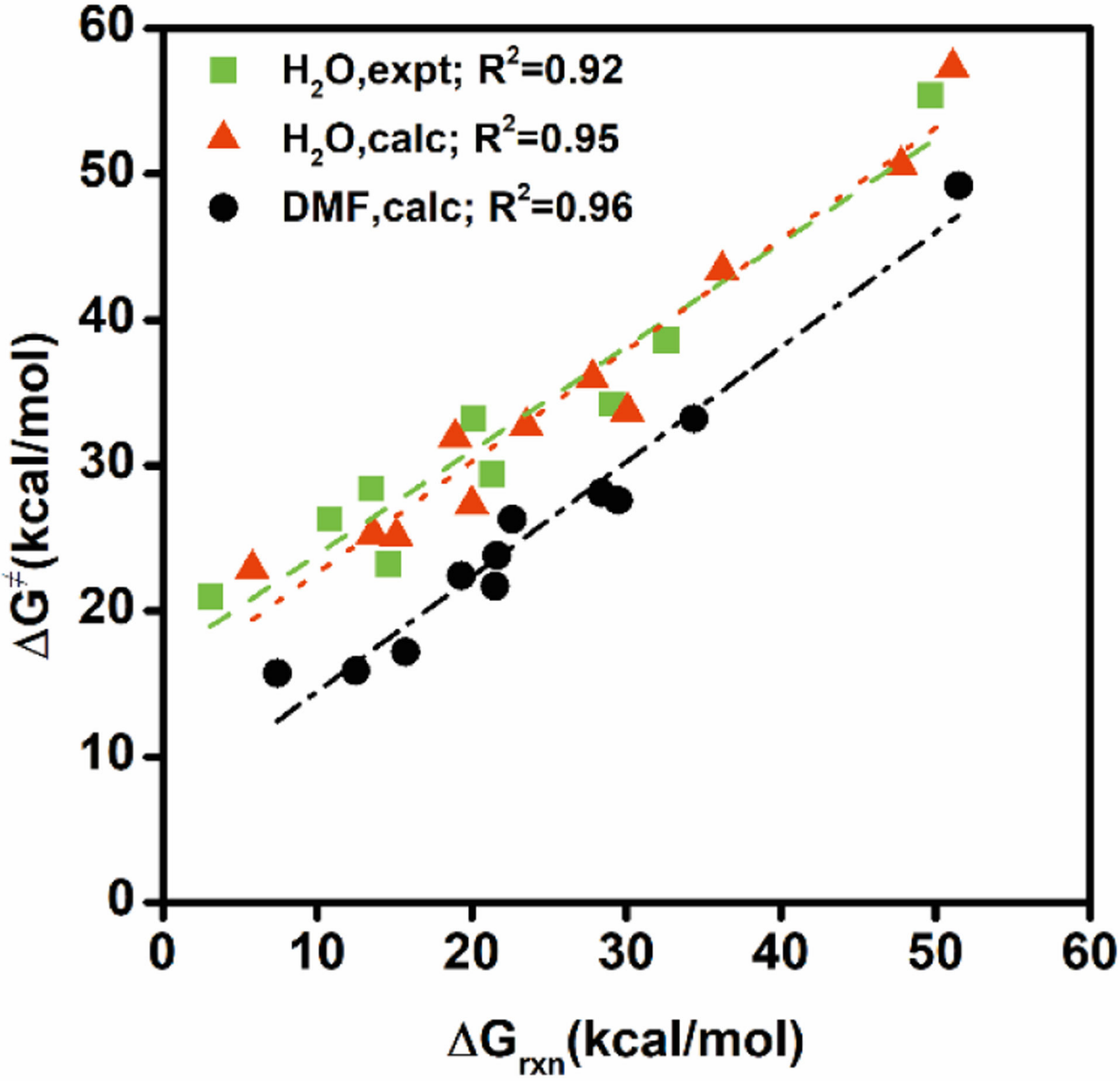

Figure 2.
Bell-Evans-Polanyi plots of computed and experimental Gibbs energies of activation for decarboxylation reactions in water and in dimethylformamide solutions versus the corresponding free energies of reactions.

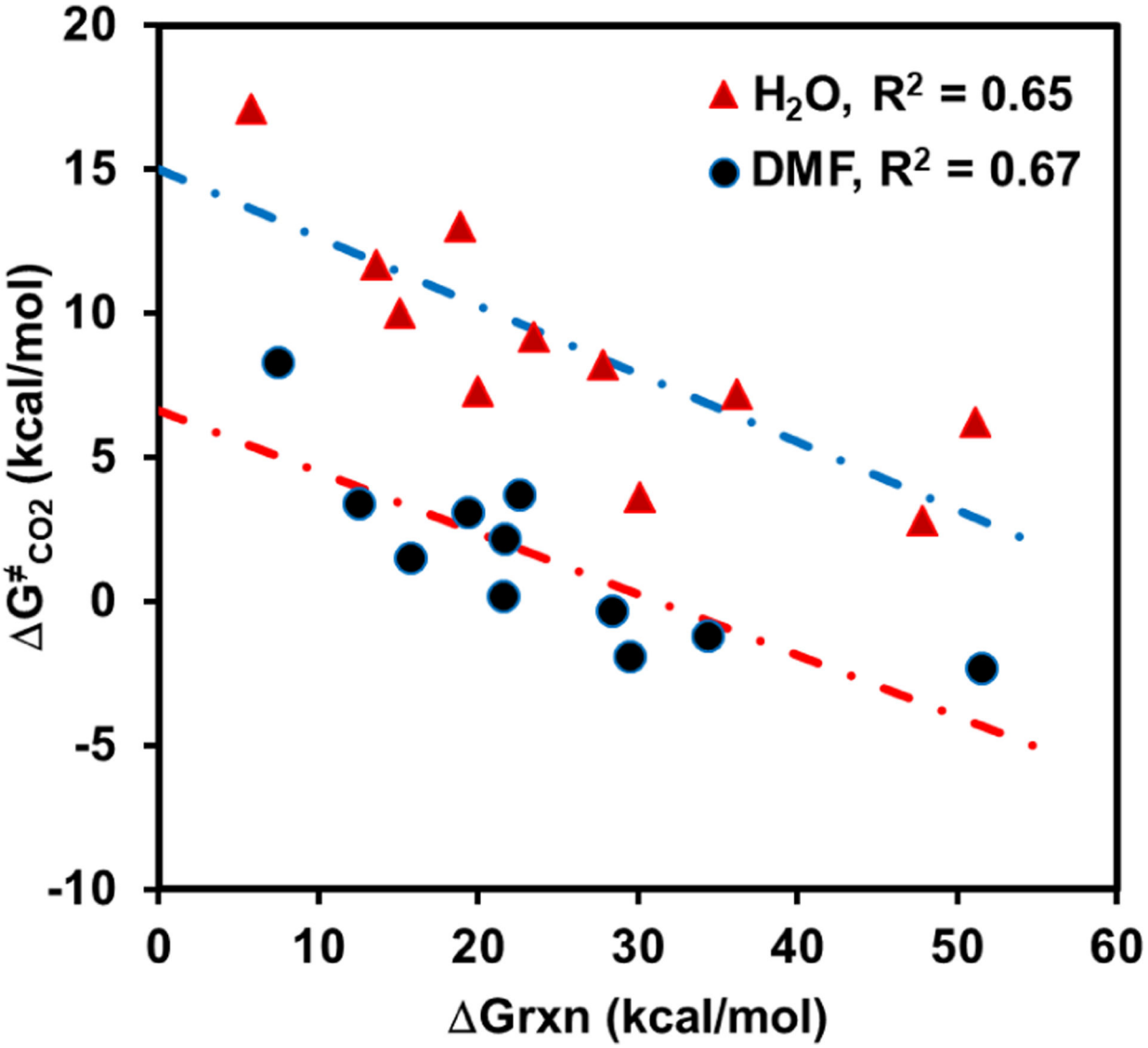

Figure 3.
Computed free energy barriers for the reverse processes of decarboxylation reactions in aqueous and in dimethylformamide solutions plotted against the corresponding free energies of reactions.

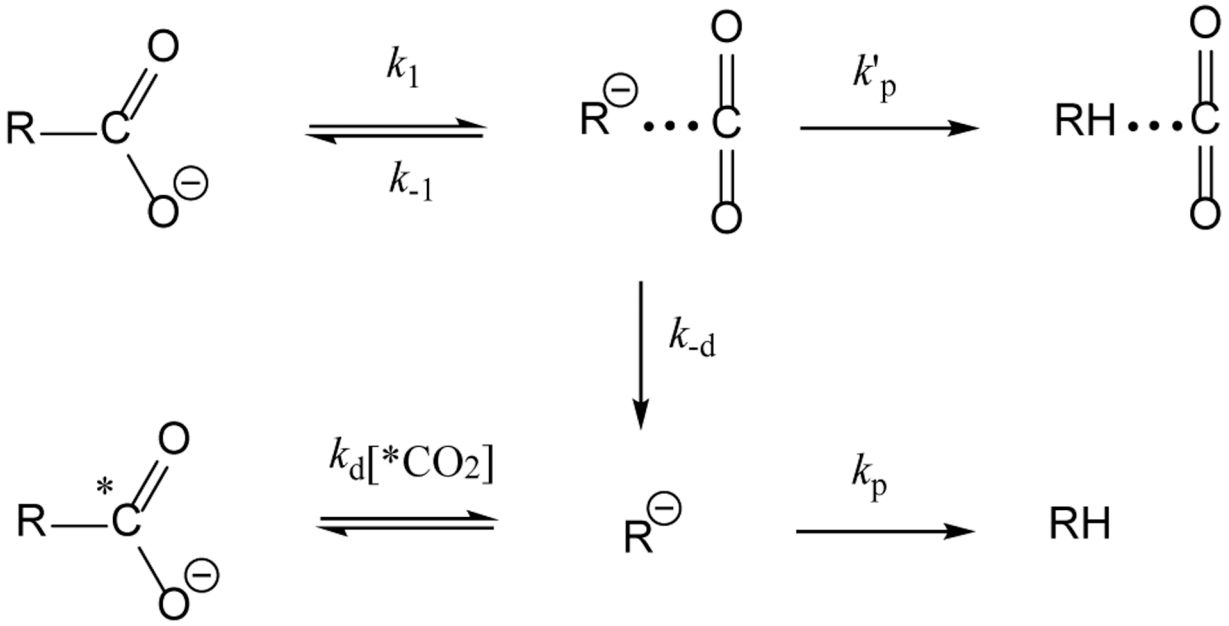

Scheme 1.

Table 1.

Calculated and experimental gas-phase basicities, and calculated free energies of reaction and barriers for the proton abstraction by the carbanion of decarboxylation from dimethylformamide, and for CO_2 recombination reactions in dimethyformamide. Geometries are optimized using M06-2X/aug-cc-pVTZ with which continuum solvation model is used for the proton transfer. All energies are given in kcal/mol.

Carbanion	Gas-phase-basicity		Proton-transfer		CO_2-recombination	
	ΔG_{cal}	ΔG_{exp}	ΔG_{rxn}^{PT}	$\Delta G_{PT}^{\neq}$	ΔG_{rxn}^{Carb}	$\Delta G_{Carb}^{\neq}$
$C_6H_5^-$	391.8	392.4	2.6	27.7	−51.5	−2.3
$C_6H_5CH_2^-$	372.6	373.8	11.9	33.0	−34.4	−1.2
p-cyanobenzyl ion	349.6	353.3	24.9	40.8	−22.6	3.7
MUA[a]	356.8	-	18.4	33.6	−29.5	−1.9
F_3C^-	369.0	370.2	22.7	34.4	−28.4	−0.3
$NCCH_2^-$	362.7	365.2	25.8	38.1	−21.5	0.2
$HO_2CCH_2^-$	361.3	361.1	24.7	39.0	−21.6	2.2
$CH_3COCH_2^-$	360.6	361.9	25.8	38.9	−19.3	3.1
Cl_3C^-	348.9	349.9	30.9	34.2[c]	−12.5	3.4
OID[b]	354.4	-	30.9	34.9[c]	−15.7	1.5
$O_2NCH_2^-$	346.3	349.7	37.1	50.4[c]	−7.4	8.3

[a] *N*-methyl-6-uracyl anion;

[b] 1-Oxoimidazolidinyl anion;

[c] transition structures were not fully optimized.